Effects of oxygen incorporation in tensile $La_{0.84}Sr_{0.16}MnO_{3-\delta}$ thin films during *ex situ* annealing

S. H. Seo, H. C. Kang,* H. W. Jang, and D. Y. Noh†
Department of Materials Science and Engineering, Gwangju Institute of Science and Technology, Gwangju, Korea
(Received 16 July 2004; revised manuscript received 27 October 2004; published 24 January 2005)

Structural changes in epitaxial $La_{0.84}Sr_{0.16}MnO_{3-\delta}$ (LSMO) (001)/$SrTiO_3$(001) thin films are studied using x-ray scattering during thermal annealing. As oxygen atoms are incorporated during annealing *ex situ* in air, the unit-cell volume contracts, which is attributed to the increased ratio of Mn^{4+} ions as indicated by enhanced saturation magnetization and ferromagnetic transition temperature. The unit-cell contraction occurs rather abruptly, suggesting that a structural phase transition happens during annealing. A 200-Å-thick film remains almost fully strained even after annealing. In this case, a fourfold structural modulation is observed which accommodates the augmented lattice strain energy.

DOI: 10.1103/PhysRevB.71.012412 PACS number(s): 75.70.Ak, 61.10.Kw, 81.65.Mq

Hole-doped lanthanum manganites $La_{1-x}A_xMnO_3$ have been intensively studied due to colossal magnetoresistance (CMR) and related interesting phenomena.[1–3] Magnetic and electrical transport properties of manganites depend on the doping level, the ratio of Mn^{4+} to Mn^{3+} ions, and the interaction between Mn^{4+}/Mn^{3+} and O^{2-} ions.[4–7] The doping level can be controlled by substituting La^{3+} by divalent ions such as Ca, Ba, and Sr,[8–10] or by tailoring oxygen stoichiometry.[11] In thin films, there are also unavoidable extra factors such as the lattice misfit strain induced by foreign substrates and oxygen deficiency. These affect the electron-lattice coupling, and thin films exhibit physical properties different from those in bulk systems.[12]

Recent studies reveal that the magnetic and transport properties of CMR thin films are substantially improved by postannealing in oxygen irrespective to the sign of lattice misfit strain.[13–15] These results are attributed to oxygen incorporation rather than to defects generation during annealing.[16] The oxygen incorporation transforms Mn^{3+} ions to Mn^{4+} with smaller ionic radius, and induce the changes in the unit-cell volume.[17]

In this experiment, we investigate the structural changes of lanthanum manganite $La_{0.84}Sr_{0.16}MnO_{3-\delta}$ (LSMO) (001) thin films grown on $SrTiO_3$ (STO) (001) substrates during postannealing in air. As the annealing proceeds, despite the oxygen incorporation, the unit cell contracts discontinuously. We attribute this to the change in the ratio of Mn^{4+}/Mn^{3+}. The increase of the saturation magnetization is consistent with the increased ratio of Mn^{4+}/Mn^{3+}. The strain in a 700-Å-thick film is relaxed completely by the annealing, and the structure changes from a tetragonal to pseudocubic structure as expected in a bulk crystal. On the other hand, a 200-Å-thick film remains almost fully strained. A fourfold structural modulation is observed, which accommodates the augmented strain energy in the 200-Å-thick film.

LSMO (001) thin films were grown epitaxially on annealed STO (001) substrates using radio-frequency (rf) magnetron sputtering technique. A conventional $La_{0.7}Sr_{0.3}MnO_3$ ceramic target of 2-in. diam was used. The composition of the films evaluated by x-ray photoelectron spectroscopy (XPS) turns out to be $La_{0.84}Sr_{0.16}MnO_{3-\delta}$, different from the nominal composition of the target. To promote the growth of the planar layer as opposed to the island growth, the STO (001) substrates were annealed at 1000 °C for 6 h, which results in large (001) terraces on the surface. During the growth, the films were kept at 610 °C and then cooled down to room temperature (RT) under 10 Torr of oxygen pressure. The surface morphology of the films are examined with atomic force microscopy (AFM) and magnetization was measured by a superconducting quantum interference device (SQUID) magnetometer.

To examine the structural changes during postannealing of the as-grown LSMO films, *in situ* synchrotron x-ray scattering measurements were performed at the beamline 5C2 at Pohang Light Source in Korea. The energy of incident x rays was fixed at 8.0 keV ($\lambda = 1.549$ Å). We selected two samples with different thickness, 200 and 700 Å, to investigate the effects of the strain as well as the annealing on the structural changes. The sample temperature was raised to 700 °C within 150 s in air, and then kept constant during the measurements.

The x-ray diffraction profile of the as-grown films show that a 200-Å-thick LSMO film is fully strained and of high quality. The LSMO (001) peak in the surface normal direction shown in Fig. 1(a) retains the interference fringes indicating that the crystalline order persists throughout the whole film thickness. The sharp diffraction peak at 1.609 $Å^{-1}$ comes from the (001) STO substrate. The in-plane (100) diffraction peak position shown in Fig. 1(b), measured using grazing incident x-ray scattering geometry, matches exactly the sharp peak of the substrate. This indicates that the film is fully strained and pseudomorphically grown. The surface of the film retains the step-terrace structure of the annealed STO substrate surface as shown in an AFM image illustrated in Fig. 1(c). The film is grown as a planar layer and the surface is quite smooth.

As the film thickness increases, the lattice strain is partially relaxed and island structure appears. The in-plane (100) peak occurs at a Q_x value larger than the substrate peak indicating partial strain relaxation. This also suggests that the in-plane lattice constant of the film, given by $a = 2\pi/Q_{peak}$, is smaller that the substrate lattice constant, and the film is under tensile stress. Upon releasing the lattice strain, the unit-cell structure becomes more tetragonally distorted. This indicates that the relaxed structure of the as-grown films is

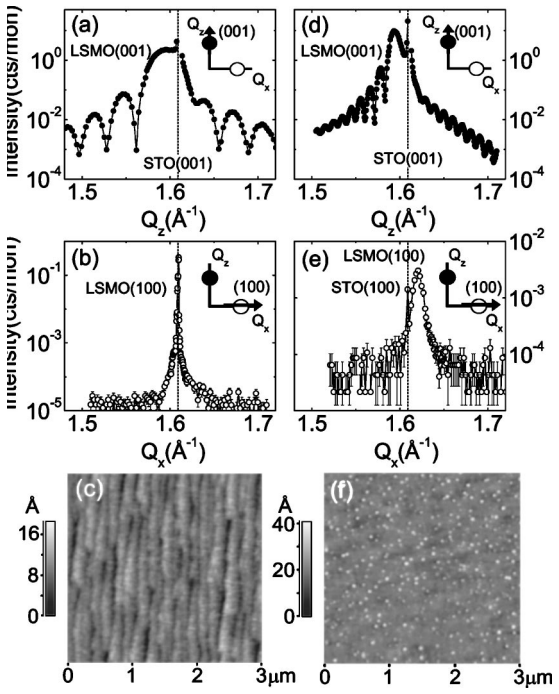

FIG. 1. Scattering profile of the as-grown LSMO (001) along the surface normal direction in (a) 200-Å-thick film and (d) 700-Å-thick film. Scattering profile of the as-grown LSMO (100) in the film in-plane direction in (b) 200-Å-thick film and (e) 700-Å-thick film. AFM images of (c) 200-Å-thick film and (f) 700-Å-thick as-grown film.

tetragonal or orthogonal with an elongated *c* axis. Oxygen deficiency must distort the oxygen octahedron in the surface normal direction. The surface consists of islands as shown in Fig. 1(f). The formation of islands can provide a route for the strain relaxation.

Figure 2(a) shows the change of the (001) peak of the 200-Å-thick film in the surface normal direction during annealing at 700 °C. The LSMO (001) occurs at a Q_z value smaller than that of the STO (001) initially. However, as the annealing proceeds it passes through the STO (001) peak and occurs at a higher Q_z value. This means that the *c*-axis lattice constant contracts during annealing. To investigate the change in the *c*-axis lattice constant as a function of annealing time quantitatively, we fit the scattering intensity profiles to a model including a LSMO film of finite thickness and a semi-infinite STO substrate. The fitting variables are the dimension of the LSMO unit cell and the interface and surface roughnesses. The results of the fitting are drawn in Fig. 2(a) in solid lines.

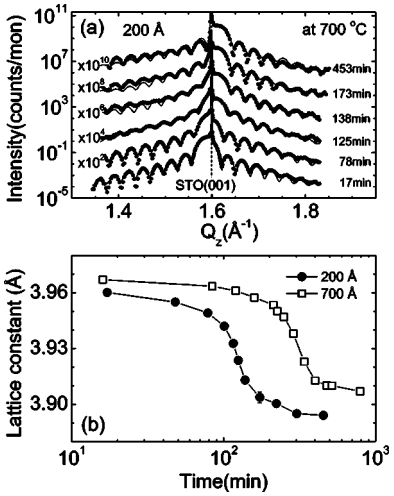

FIG. 2. (a) Scattering profiles of the LSMO (001) in the surface normal direction during annealing. The solid lines are the results of fit. (b) *C*-axis lattice spacing as a function of annealing time. The solid line is a guide to the eye.

The behavior of the *c*-axis lattice constant obtained from the fit is illustrated in Fig. 2(b). We note that in the 200-Å-thick film, the in-plane *a*-axis constant stays constant matching to the substrate lattice indicating that the film remains fully strained during the annealing. Therefore, Fig. 2(b) suggests that the unit-cell volume decreases while more oxygen is incorporated in the film. We attribute this to the conversion of Mn^{3+} to Mn^{4+} ions. During postannealing, oxygen atoms diffuse into the film and compensate oxygen vacancies rather than occupying interstitial sites in perovskite structure.[18] Considering the charge balance, such oxygen incorporation would transform Mn^{3+} ions into Mn^{4+} with a smaller ionic radius that lessens the distortion of the oxygen octahedron and decreases the unit cell.

The *c*-axis lattice constant decreases rather abruptly during annealing as shown in Fig. 2(b). There is little change in the *c*-axis lattice constant until the annealing time reaches 100 min. As the annealing time reaches to about 100 min, it suddenly decreases in a few minutes, and saturates close to the final value. This is in contrast to the typical thermal oxidation process, where one expects a parabolic or logarithmic increase of the oxygen content as the annealing time increases.[19] The behavior of the *c*-axis lattice constant indicates that a structural phase transition, probably from a tetragonal to pseudocubic structure, occurs as the oxygen atoms are incorporated resulting in electron transfer between the oxygen and manganese ions. In the 200-Å-thick film, however, the *c*-axis lattice constant becomes even smaller than the *a*-axis lattice constant due to the lattice strain. In bulk $La_{1-x}Sr_xMnO_3$, transitions between orthorhombic and rhombohedral phases occur near $x=0.17$, and can be induced by the dopant concentration.[8]

On the other hand, the partially strain relaxed 700-Å-thick film becomes pseudocubic after annealing. This indicates that the strain is progressively relaxed as more oxygen ions are incorporated in the lattice. Although we cannot estimate

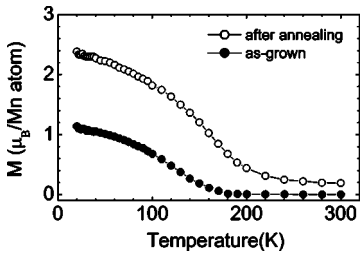

FIG. 3. Temperature dependence of the magnetization of the as-grown and the annealed LSMO films.

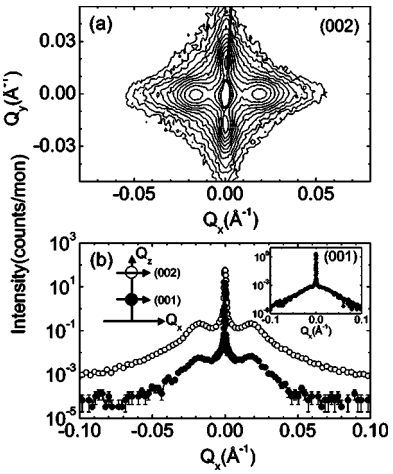

FIG. 4. Satellite peaks observed near the LSMO (001) peak of the annealed 200-Å-thick film. The inset shows that the satellite peaks occur at identical in-plane positions.

the evolution of lattice strain quantitatively due to the lack of relaxed lattice parameters of the film, it is likely that the strain is mostly relaxed during the transition to the pseudocubic structure.

The increased ratio of Mn^{4+}/Mn^{3+} is reflected in the magentic properties of the annealed films. Figure 3 shows the magnetization of the 700-Å-thick film measured under a magnetic field of 1 T before and after the annealing. The saturation magnetization is almost doubled and the ferromagnetic transition temperature is increased from about 130–180 °C. These facts are consistent with the generic bulk phase diagram where the ferromagnetic phase is enhanced by increased Mn^{4+} fraction.[8]

Finally, we note that there appear satellite peaks near the Bragg peaks after annealing. As shown in Fig. 4, the satellite peaks appear along the crystallographic $[\pm 100]$ and $[0 \pm 10]$ directions in the film plane exhibiting fourfold symmetry. The satellite peaks near the (001) and (002) Bragg reflections occur at identical in-plane positions as shown in the inset of Fig. 4. This excludes often observed microtwinning as the origin of the satellite peaks, and indicates that the atomic structure of the film is modulated with the period of about 350 Å ($=2\pi/\Delta Q$) in the film plane direction. Although the origin of this modulation is not clear at this moment, it is likely that a periodic domain structure is formed to accommodate the augmented strain energy after annealing. The satellite peaks are not observed in a 700-Å-thick film, which exhibits strain-relaxed pseudocubic structure after annealing.

Studying the effect of lattice strain by replacing $SrTiO_3$ substrate with $LaAlO_3$ or by reducing the oxygen pressure during growth would cast some clues to the structural behavior of the LSMO film during oxygen incorporation. $LaAlO_3$ substrate induces compressive strain, and oxygen incorporation would reduce the lattice strain in this case. Reducing the oxygen content during the growth would increase the lattice spacing of the LSMO/STO film. This will increase the critical thickness. Films thicker than 200 Å would exhibit behavior similar to that observed on the 200-Å film in this experiment.

In summary, we measured the structural changes of epitaxial $La_{0.84}Sr_{0.16}MnO_{3-\delta}$ (LSMO) (001)/$SrTiO_3$(001) films during postannealing by *in situ* x-ray scattering. Magnetic properties of the films are substantially enhanced due to the increased ratio of Mn^{4+}/Mn^{3+}. The *c*-axis lattice constants decreases rather abruptly as the film is annealed indicating that a structural phase transition from tetragonal to pseudocubic might occur.

The authors thank Jong-Soo Rhyee and B. K. Cho for their help in measuring the magnetic properties. This work was supported by MOST through the National Research Laboratory (NRL) Program on Synchrotron X ray and X-ray/Particle-beam Nanocharacterization. The PLS is supported by the Korean Ministry of Science and Technology.

*Present address: Argonne National Laboratory, Argonne, IL 60439.
†Electronic address: dynoh@kjist.ac.kr

[1] S. Jin, T. H. Tiefel, M. McCormack, R. A. Fastnacht, R. Ramesh, and L. H. Chen, Science **264**, 413 (1994).
[2] C. H. Chen and S.-W. Cheong, Phys. Rev. Lett. **76**, 4042 (1996).
[3] H. Kawano, R. Kajimoto, H. Yoshizawa, Y. Tomioka, H. Kuwahara, and Y. Tokura, Phys. Rev. Lett. **78**, 4253 (1997).
[4] C. Zener, Phys. Rev. **82**, 403 (1951).
[5] J. B. Goodenough, Phys. Rev. **100**, 564 (1955).
[6] P.-G. de Gennes, Phys. Rev. **118**, 141 (1960).
[7] W. Prellier, Ph. Lecoeur, and B. Mercey, J. Phys.: Condens. Matter **13**, R915 (2001).
[8] A. Urushibara, Y. Moritomo, T. Arima, A. Asamitsu, G. Kido, and Y. Tokura, Phys. Rev. B **51**, 14 103 (1995).
[9] P. Schiffer, A. P. Ramirez, W. Bao, and S.-W. Cheong, Phys. Rev. Lett. **75**, 3336 (1995).
[10] H. Y. Hwang, S.-W. Cheong, P. G. Radaelli, M. Marezio, and B. Batlogg, Phys. Rev. Lett. **75**, 914 (1995).
[11] H. L. Ju, J. Gopalakrishnan, J. L. Peng, Qi Li, G. C. Xiong, T. Venkatesan, and R. L. Greene, Phys. Rev. B **51**, 6143 (1995).
[12] S. Jin, T. H. Tiefel, M. McCormack, H. M. O'Bryan, L. H. Chen, R. Ramesh, and D. Schurig, Appl. Phys. Lett. **67**, 557 (1995).
[13] R. von Helmolt, J. Wecker, B. Holzapfel, L. Schultz, and K. Samwer, Phys. Rev. Lett. **71**, 2331 (1993).
[14] D. Cao, F. Bridges, D. C. Worledge, C. H. Booth, and T. Geballe, Phys. Rev. B **61**, 11 373 (2000).
[15] P. Murugavel, J. H. Lee, J.-G. Yoon, T. W. Noh, J.-S. Chung, M. Heu, and S. Yoon, Appl. Phys. Lett. **82**, 1908 (2003).
[16] J. R. Sun, C. F. Yeung, K. Zhao, L. Z. Zhou, C. H. Leung, H. K. Wong, and B. G. Shen, Appl. Phys. Lett. **76**, 1164 (2000).
[17] W. Prellier, M. Rajeswari, T. Venkatesan, and R. L. Greene, Appl. Phys. Lett. **75**, 1446 (1999).
[18] J. A. M. van Roosmalen and E. H. P. Cordfunke, J. Solid State Chem. **110**, 109 (1994).
[19] D. A. Jones, *Principles and Prevention of Corrosion*, 2nd ed. (Prentice Hall International, Singapore, 1997).